Applied Radiation and Isotopes 163 (2020) 109211

Contents lists available at ScienceDirect

Applied Radiation and Isotopes

journal homepage: http://www.elsevier.com/locate/apradiso

Preparation and characterization of poly nano-cerium chloride for ^{99}Mo production based on neutron activation reactions

M.I. Aydia [a], A.S. Hiekal [a], K.M. El-Azony [a,*], T.Y. Mohamed [b], I.M. Shahin [b]

[a] Radioactive Isotopes and Generator Department, Hot Labs Center, Atomic Energy Authority, P.O. 13759, Cairo, Egypt
[b] Faculty of Science, Benha University, P.O. Box 13518, Benha, Egypt

ARTICLE INFO

Keywords:
Poly nono cerium chloride
PNCC
^{99}Mo
Molybdate
Exchange reaction

ABSTRACT

Different molar ratios of the cerium trichloride heptahydrate to isopropyl alcohol (1:2, 1:3 and 1:5) were studied to choose the optimum ratio, and studied the reaction temperature effect (80, 90 and 100 °C) to determine the optimum temperature for the preparation of poly nano cerium chloride (PNCC). The PNCC-1 was selected among the prepared PNCC batches based on the ^{99}Mo sorption properties that confirms the feasibility of using it as a novel effective sorbent material. The structural properties and chemical composition were studied using different techniques and devices such as EDX, XRD, FESEM, FTIR, TGA, and DTA. The sorption capacity was found to be 450 ± 27 and 195 ± 11 mg/g PNCC-1 using the static and dynamic techniques, from 0.01 M NaOH to obtain about 55 and 75% ^{99m}Tc separation efficiency, respectively. The acceptability of the eluate ^{99m}Tc was investigated from the point of view of radiochemical, radionuclidic and chemical purity.

1. Introduction

Technetium-99m is a short-lived meta-stable nuclear isomer [Seaborg and Segrè, 1939] and is commonly used for diagnostic purposes in nuclear medicine, where more than 80% of all nuclear medicine procedures are diagnostic applications and more than 85% of the images are used it because of the suitability of its chemical and nuclear properties ($T_{1/2}$ = 6.01h; monoenergetic γ-ray, E_γ = 140 keV; I_γ = 89.4%) [Boyd, 1982; IAEA, 2008; Boyd, 1997; Zolle, 2007; Eckelman, 2009; Lee et al., 2016]. ^{99m}Tc is produced from the ^{99}Mo decay ($T_{1/2}$ = 65.94 h) used in the preparation of the column generator [Zolle, 2007; Eckelman, 2009]. The fission ^{99}Mo is produced with a high specific activity ~370 TBq (104 Ci/g) and low uptake capacity on alumina. (2–20 mg Mo/g) [Molinsky, 1982; Evans and Shying, 1984; Eckelman and Coursay, 1982]. The availability of fission ^{99}Mo is a major challenge, as advanced technology is required to overcome high levels of radioactive waste and provide medical grade ^{99m}Tc [Perkins and Vivian, 2009 . Gould, 2009; Cecchin et al., 2010; Ballinger, 2010]. Several studies have been done to minimize dependence on the fission ^{99}Mo, either through charged particle nuclear reactions or neutron activation reactions. Accelerator-based production methods were studied and proposed as potential alternatives for ^{99m}Tc production, whether directly produced or by the β^- decay of ^{99}Mo using ^{100}Mo(p,2n)^{99m}Tc or ^{100}Mo(p,pn)^{99}Mo, respectively [Lagunas-Solar et al., 1991; Lagunas-Solar, 1993; Scholten et al., 1999; Takács et al., 2003; Pupillo et al., 2015]. The neutron activation reaction was used to produce ^{99}Mo using thermal neutrons (σ = 0.13 b) with a low or medium-specific activity (50–500 GBq/g) [Evans and Shying, 1984; Monroy-Guzman et al., 2007]. The epithermal neutrons with high integral resonance energy cross section (σ = 7.2 b) were used to increase the specific activity of ^{99}Mo. [Parrington et al., 1996]. According to the latest data, the global demand is approaching 9500 Ci 12000 Ci " 6 d C ″ ^{99}Mo per week, further growth is expected [NEA, 2018]. Unfortunately, the low yield of ^{99}Mo produced by the charged particle reactions has led to believe that using the neutron activation reactions and the creation of new substances with high capacity for ^{99}Mo adsorption is the ideal alternative method. To increase the ^{99}Mo uptake capacity onto the exchanger with taking into account an elution yield, chemical and radionuclidic purity of ^{99m}Tc. Tanase et al., (1997) reported that the polymeric zirconium compound (PZC) was used with a high sorption capacity of ^{99}Mo (198.7 ± 10 mg/g) however, sadly, the ^{99}Mo breakthrough is relatively high (<0.5%) according to the United States Pharmacopoeia, which indicates a molybdenum percentage of less than 0.015% in ^{99m}Tc. From 2008 to 2019, Rubel Chakravarty et al., began developing ^{99}Mo/^{99m}Tc generators based on the preparation of several new exchanges such as polynano Titania, Nano-Zirconia, Nanocrystalline γ-Al_2O_3, Mesoporous Alumina (MA), Mesoporous

* Corresponding author.
E-mail address: azonychemist@gmail.com (K.M. El-Azony).

https://doi.org/10.1016/j.apradiso.2020.109211
Received 28 June 2019; Received in revised form 28 April 2020; Accepted 29 April 2020
Available online 23 May 2020

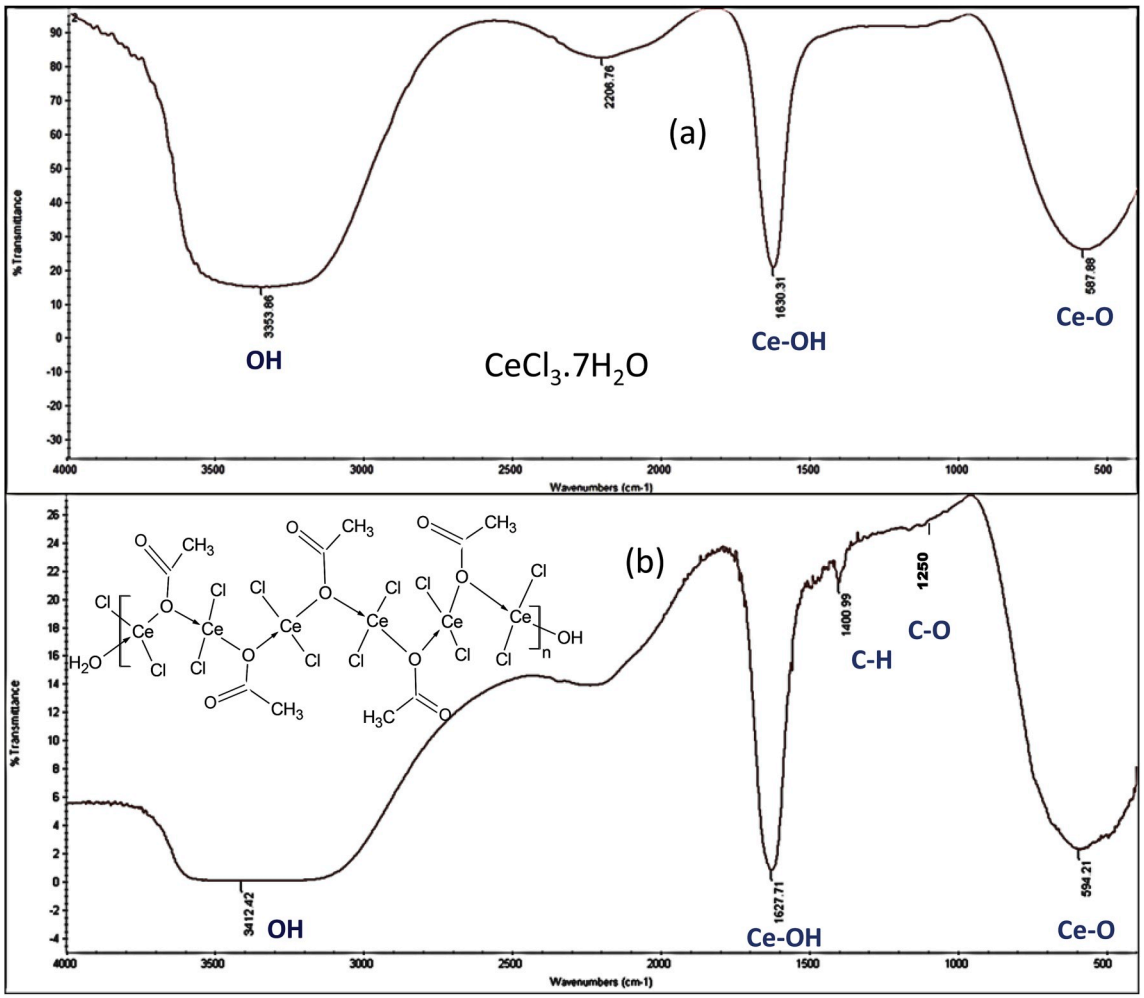

Fig. 1. IR spectrum of (a)$CeCl_3{\cdot}7H_2O$, (b)PNCC-1.

Al_2O_3 nanospheres and Mesoporous Alumina [Chakravarty et al., 2008; Chakravarty et al., 2010 Chakravarty et al., 20012; Chakravarty et al., 2013; Saptiama et al., 2018; Chakravarty et al., 2019]. They have successfully improved the sorption capacity of ^{99}Mo, with an acceptable ^{99m}Tc elution yield and ^{99}Mo breakthrough, under dynamic conditions from 75 to 251 mg Mo per g from polynano titania to mesoporous alumina, respectively. The use of high temperatures at 600 °C during the preparation process of mesoporous alumina affects the crystal size and is found to be 2–4 nm, which may be affected to use in large-scale column applications. The cross-linked chitosan polymer for the formation of microporous composite materials (MPCM) has excellent selectivity for molybdenum with a high sorption capacity, while the pertechnate ion is passed through a saline solution with an efficiency of more than 75% [Chattopadhyay et al., 2017; Hasan, 2014]. In general, the reaction preparation procedure requires long periods, respectively ranging from 4 to about 8 h and also need an additional alumina column to purify ^{99m}Tc from ^{99}Mo.

In this study, poly nano cerium chloride was simply prepared as a prospective material for the ^{99}Mo/^{99m}Tc generator by studying the reaction conditions of the PNCC preparation, characterizing the chosen compound, assessing its sorption properties and a preliminary study of the chosen PNCC matrix for application in the ^{99}Mo/^{99m}Tc generator.

2. Experimental

2.1. Chemicals and reagents

Most of the chemicals used are analytical grade. Double distilled water (DDW) was used.Molybdenum oxide (MoO_3), sodium hydroxide (NaOH), sodium chloride (NaCl), cerium trichloride heptahydrate ($CeCl_3{\cdot}7H_2O$), isopropyl alcohol and acetone were purchased from Merck, Germany.

2.2. Preparation of poly nano cerium chloride (PNCC)

PNCC was prepared by studying various factors affecting the preparation of stable and selective inorganic polymer for ^{99}Mo such as the molar ratio of cerium trichloride heptahydrate ($CeCl_3{\cdot}7H_2O$) to isopropyl alcohol (IPrOH) (1:2; 1:3 and 1:5), the reaction temperature (80, 90 and 100 °C) within 3 h, then increased to 160 °C for 1h. PNCC compounds are prepared to study molar ratios by adding 60 g of $CeCl_3{\cdot}7H_2O$ to 24.4, 36.7 and 61.2 ml of IPrOH that refers to 1:2; 1:3 and 1:5, respectively. The 1:2 M ratio solution was stirred and condensed by raising the temperature for 3 h to study the different temperatures (80, 90, 100 °C); the solution was viscous and then converted into an insoluble polymer slurry by raising the temperature to 160 °C for 1 h, then left to cool and solidify at room temperature.

2.2.1. Preparation of poly nano cerium chloride-1 (PNCC-1)

PNCC-1 was prepared using the 1:2 M ratio of $CeCl_3{\cdot}7H_2O$ to IPrOH,

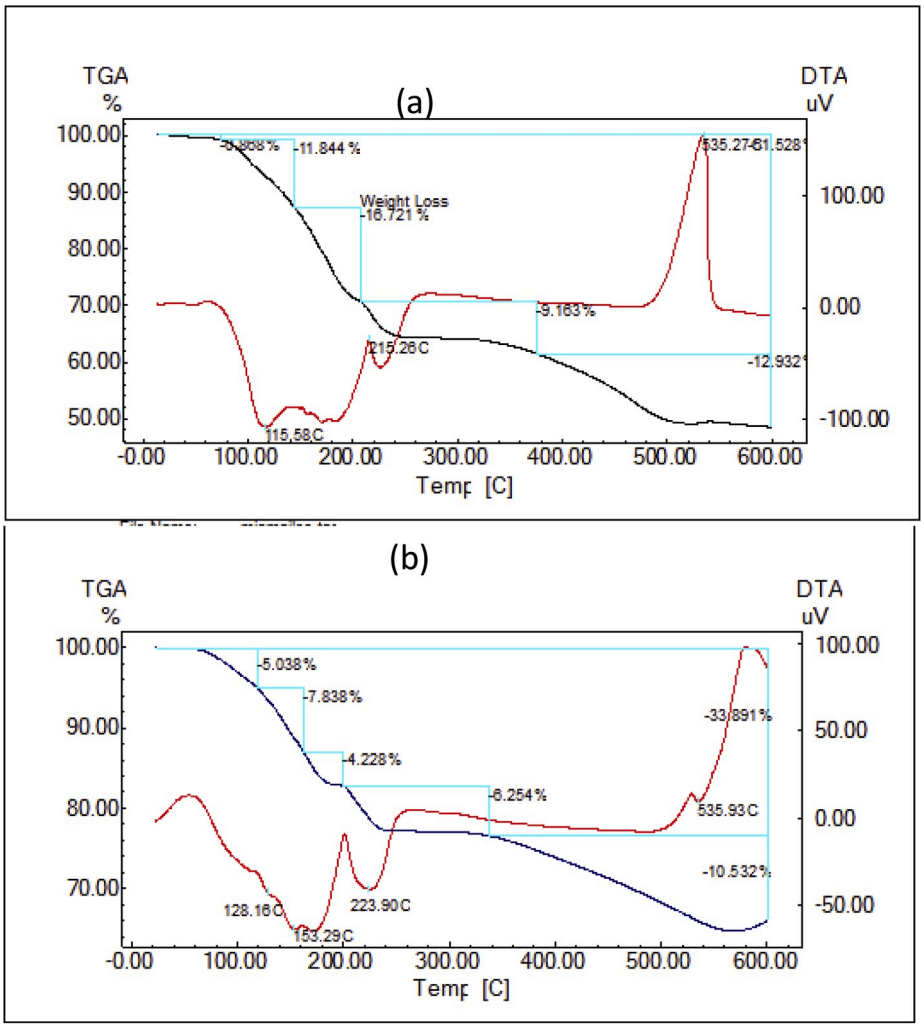

Fig. 2. TGA and DTA curves for (a)$CeCl_3{\cdot}7H_2O$ and (b)PNCC-1.

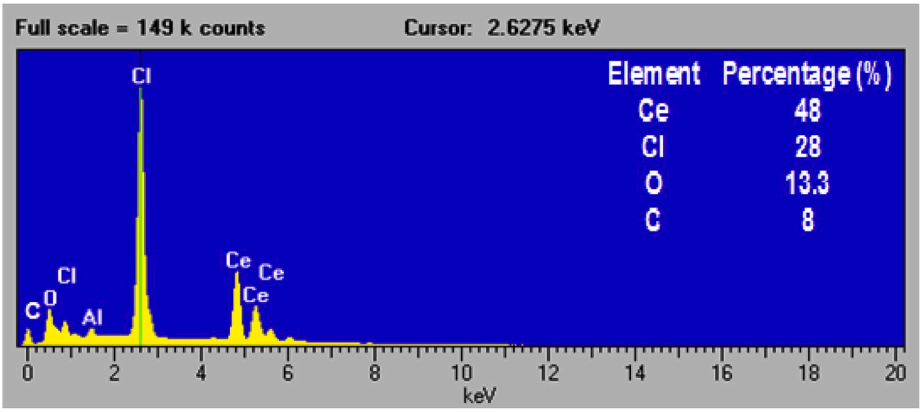

Fig. 3. EDX spectrum of the polynano cerium chloride (PNCC-1).

then raising the temperature of the reaction to 90 °C for 3 h. The solution became viscous and transformed by raising the temperature to 160 °C for an hour to an insoluble polymer slurry, then allowed to cool and solidify at the room temperature.

2.3. Characterization of PNCC-1

Various techniques and devices were used to characterize the PNCC-1. Energy dispersive X-ray (SEM-EDX, JSM 5600, JEOL) was used to determine the chemical composition of PNCC-1 (cerium, chlorine, oxygen, and carbon concentrations). The elemental analysis was used to determine the concentration of hydrogen. Fourier Transform Infra-Red (FTIR) spectrometer (Bomem, Model MB157S, Canada) ranged from 4000 to 400 cm^{-1} and used KBr disk method to determine PNCC-1 functional groups. Thermal analysis was used to study the thermal stability of PNCC-1 at a heating rate of 15 min under a nitrogen atmosphere

Strongest 3 peaks

no. peak no.	2Theta (deg)	d (A)	I/I1	FWHM (deg)	Intensity (Counts)	Integrated Int (Counts)
1 64	26.1885	3.40008	100	0.13710	32	272
2 61	25.1050	3.54431	75	0.19000	24	249
3 34	15.1050	5.86071	69	0.17000	22	214

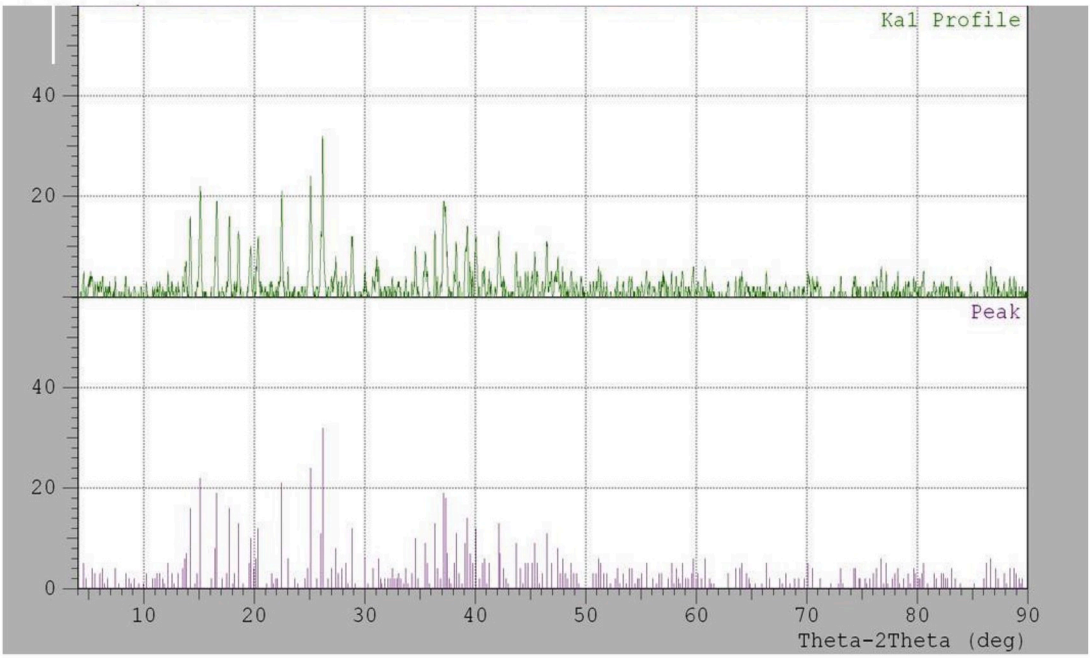

Fig. 4. XRD pattern of PNCC-1 particles.

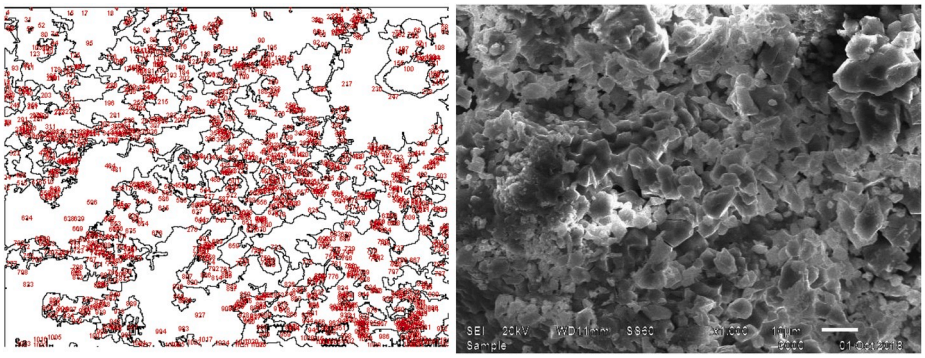

Fig. 5. SEM photography of PNCC-1 nano and micro-particle exchanger.

using Shimadzu DT-60, Japan. The morphological structure was investigated using a field emission scanning electron microscope (FESEM), model JSM-6510°A, Japan. PNCC-1 X-ray diffraction pattern (XRD) was recorded using Bruker spectrometer, model D8 Advance, USA with 18 keV diffractometer and monochromatic CuK_{α} radiation ($\lambda = 1.54178$ °A) to determine its crystalline structure. An energy-dispersive X-ray spectrometer (XRF), analyzer JSX-3222, Japan (type JEOL), used to determine the concentration of adsorbed molybdenum.

2.3.1. Acid-base titration of PNCC-1

Samples of 100 mg of PNCC-1 were placed in 20 ml glass vials, divided into two series and equilibrated with different volume ratios of 0.1 M NaCl/0.1 M HCl and 0.1 M NaCl/0.1 M NaOH at 25 ± 1 °C for 24 h, with maintaining a total volume of 10 ml and constant ionic strength (0.1 M) in each vial. In order to determine the acid-base titration curve, the pH values of the equilibrated solutions were measured and plotted against the added meq H^+/g PNCC-1and meq OH^-/g PNCC-1. Then the same technique was used to determine the blank titration curve without using PNCC-1.

2.3.2. Chemical stability

Approximately 185 kBq (5 μCi) of ^{141}Ce ($T_{1/2} = 32.5$ d; $E_{\gamma} = 145.44$ keV; $I_{\gamma} = 48.2\%$) were added to $CeCl_3{\cdot}7H_2O$ during PNCC-1 preparation as described in section (2.2.1). 100 mg of $PN^{141}CC$-1 equilibrated at room temperature with 10 ml of varying NaOH concentrations for 24 h. The centrifugation technique separated the NaOH solution from the labeled [^{141}Ce] -PNCC-1 matrix. The liquid and solid phases were measured using the HPGe detector connected to the multichannel analyzer to determine the ^{141}Ce level.

2.3.3. Determination of the PNCC-1 empirical formula

The energy dispersive X-ray (EDX) was used to determine the proportions of the chemical constituents of PNCC-1 for calculating the empirical formula. The number of moles of each element was calculated

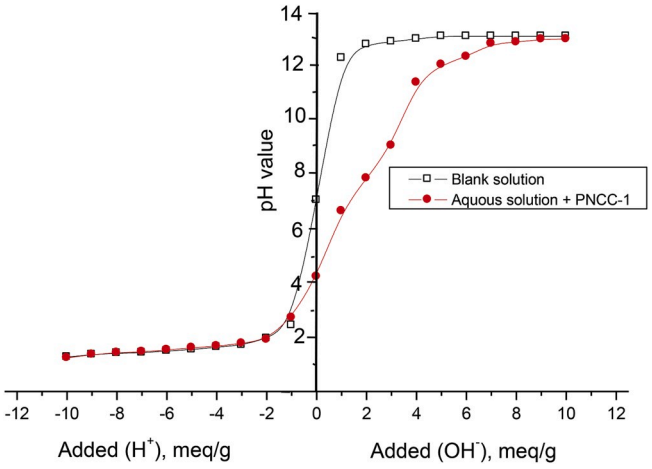

Fig. 6. Acid-base titration curve of PNCC-1.

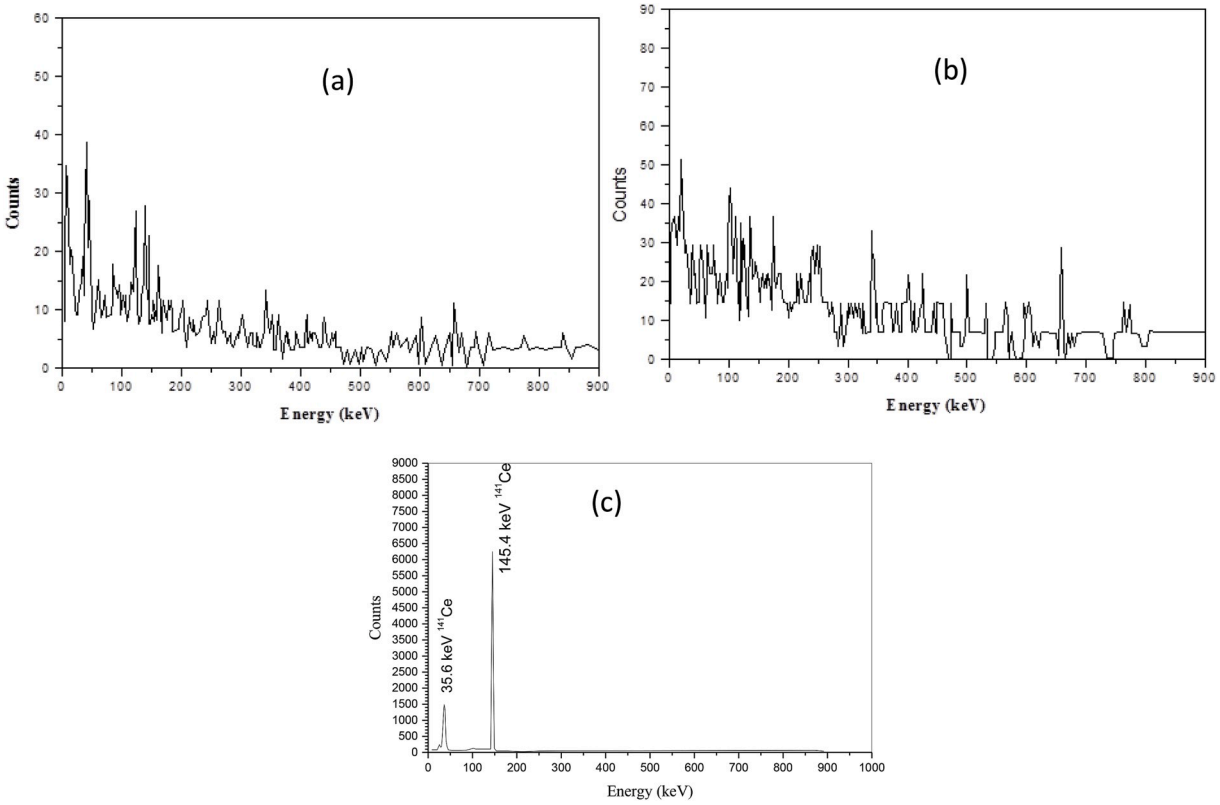

Fig. 7. Gamma-ray spectra for liquid phase of (a)0.1M NaOH or (b)1M NaOH and (c)the solid phase 100 mg of [^{141}Ce]-PNCC-1.

Table 1
The effect of molar ratio of cerium chloride to isopropyl alcohol at 90 °C on the ^{99}Mo uptake capacity and ^{99m}Tc separation yield using static technique (n = 3).

Exchanger No	Molar ratio of $CeCl_3 7H_2O$: IPrOH	Static technique		Dynamic technique	
		Adsorption capacity of Mo (mg g^{-1} PNCC)	Separation yield of ^{99m}Tc %	Adsorption capacity of Mo (mg g^{-1} PNCC)	Elution yield of ^{99m}Tc (%)
PNCC-1	1:2	450±27	54±3	195 ± 11	75 ± 5
PNCC-2	1:3	393±20	27±15		
PNCC-3	1:5	355±18	31±2		

Table 2
The effect of temperature on the uptake capacity of Mo and the ^{99m}Tc separation yield using a constant molar ratio (1:2) of cerium chloride to isopropyl alcohol and static technique (n = 3).

Exchanger No	Reaction temperature (°C)	Static technique		Dynamic technique	
		Adsorption capacity of Mo (mg g^{-1} PNCC)	Separation yield of ^{99m}Tc %	Adsorption capacity of Mo (mg g^{-1} PNCC)	Elution yield of ^{99m}Tc (%)
PNCC-1	90	450±27	54±3	195 ± 11	75 ± 5
PNCC-4	80	410±22	49±1.2		
PNCC-5	100	430±25	52±1.4		

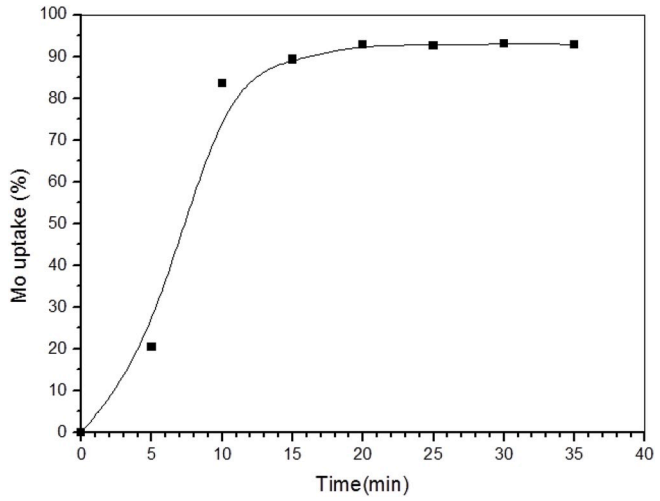

Fig. 8. Percentage uptake of 0.01M^{99}Mo-molybdate (VI) as a function of contact time (using 0.01 M NaOH and PNCC-1 matrix).

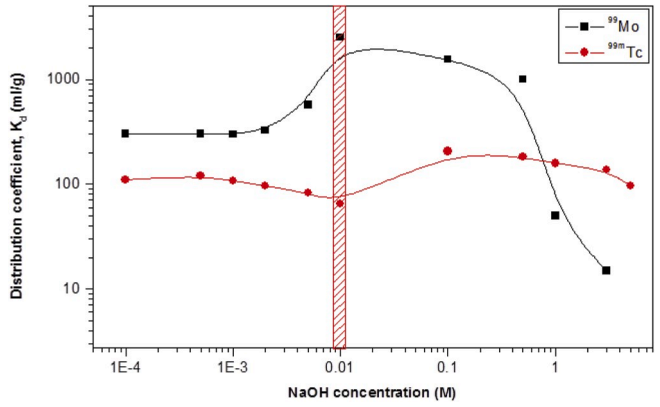

Fig. 9. Effect of NaOH concentration on the *Kd* of ^{99}Mo and ^{99m}Tc for the PNCC-1 matrix, using reasonable amount of ^{99}Mo in 0.01M molybdate(VI) and ^{99m}Tc.

by dividing the proportion of each element exist in PNCC-1 on its mass number. Then to determine the empirical formula, the calculated mole number for each element was divided by the least mole number exist in PNCC-1. The FTIR spectrum used to verify the validity of the empirical formula by evaluating the functional groups in the PNCC-1.

2.4. Molybdenum-99 solution and cerium-141

Low-enriched uranium (19.75%) irradiation at the Second Egyptian Research Reactor (ETRR-II) was performed by a neutron flux of 1×10^{14} n cm^{-2} s^{-1} for the period of 48 h to produce and separate ^{99}Mo in 2 M NaOH solution. A suitable amount of molybdenum-99 was supplied from Radioisotope Production Facilities (RPF), the Atomic Energy Authority, Egypt. A few drops of ^{99}Mo 3.7–7.4 GBq (100–200 mCi) were diluted by adding 0.01 M molybdenum solution as a carrier in 0.01 M NaOH to study the adsorption behavior of ^{99}Mo and ^{99m}Tc on the PNCC-1 matrix as a prospective material for the ^{99}Mo/^{99m}Tc generator.

Approximately 185 kBq (5 μCi) of cerium-141 were obtained as a gift from the Department of Nuclear Chemistry, Atomic Energy Authority, Egypt.

2.5. Ion exchange method

In order to optimize the separation process by batch technique, the adsorption behavior of ^{99}Mo and ^{99m}Tc on the PNCC-1 matrix from different NaOH concentrations was studied. 100 mg of the PNCC-1 matrix was placed in a clean glass vial and 10 ml of different NaOH concentrations containing 10 mg Mo spiked with a suitable amount of ^{99}Mo ~370 kBq (10 μCi) were added. The mixture was shaken at different time intervals to determine the equilibrium time. In this study the concentrations of NaOH used are 0.0001, 0.0005, 0.001, 0.002, 0.01, 0.05, 0.1, 0.5, 1, 3 and 5 M. PNCC-1 was left to settle down; 1 ml from the aqueous phase was drawn to measure ^{99}Mo and ^{99m}Tc. The distribution coefficients (K_d) of MoO_4^{2-} and TcO_{4-} were determined by using the following equation:

$$K_d = \frac{(A_o - A_e)}{A_e} \times \frac{V}{m} \qquad \left(\frac{ml}{g}\right)$$

where A_o and A_e are the counting rates of the aqueous phase before and after the equilibration, respectively, were measured. V is the total volume of the aqueous phase (ml), m is the weight of the PNCC-1 matrix (g). The equilibrium time of ^{99}Mo sorption on the PNCC-1 matrix was determined at different time intervals (5–40 min). To confirm the validity of the reaction mechanism and demonstrate that the two chloride ions substituted by molybdenum ion (MoO_4^{2-}) in PNCC-1. The steps were carried out by the following order:

- The elemental analysis device (XRF) was used to evaluate and compare the chemical composition of the PNCC-1 as an exchanger before and after Mo adsorption.
- 100 mg of the PNCC-1 was placed in a 20 ml glass vial.
- 10 ml molybdenum solution (1 mg/ml) in 0.01M NaOH was added to the PNCC-1 for 35 min.
- The solid phase was separated from the aqueous phase by filtration, washed using 0.01M NaOH and dried at the 50 °C for 24 h.
- The constituents of PNCC-1 were then assigned again using the elemental analysis (XRF).

2.5.1. Sorption capacity

The sorption capacity of molybdenum on the PNCC-1 was evaluated in both static and dynamic conditions. Firstly, batch equilibration technique (static conditions) was used to determine the uptake capacity of molybdenum on PNCC-1 matrix. 10 ml of sodium molybdate solution (8 mg/ml) dissolved in 0.01M NaOH. This solution of 80 mg Mo was labeled with ^{99}Mo ~370 kBq (10 μCi), then added 100 mg of PNCC-1 to the glass vial. The mixture was kept in a shaker for 35 min at room

Table 3
Determination of Mo sorption capacity on PNCC-1 by static and dynamic techniques, then comparison of the ^{99m}Tc elution yield with the poly nano metal oxides.

Matrix	Static sorption capacity	Dynamic sorption capacity	Elution yield of ^{99m}Tc	^{99}Mo breakthrough	References
	mg Mo/g sorbent	mg Mo/g sorbent	(%)	(%)	
poly zorconium chloride	Not performed	198.7±10.1	80	<0.00001	Tanase et al. (1997)
Poly nano Titania (TiP)	115	75	80	<0.001	Chakravarty et al. (2008)
Nano-Zirconia	250±10	80	>85	<0.0001	Chakravarty et al. (2010)
Nanocrystalline γ-Al2O3	205± 10	156±6	>80	<0.01	Chakravarty et al. (2012)
Mesoporous Alumina (MA)	225±20	168±12	55–60	0.002–0.005	Chakravarty et al. (2013)
Mesoporous Al_2O_3 nanospheres	56.2	Not performed	Not performed	Not detected	Saptiama et al. (2018)
Mesoporous alumina	391±12	251±13	>80	0.002–0.004	Chakravarty et al. (2019)
PNCC-1	450±28	195±11	~75	0.003–0.008	This work

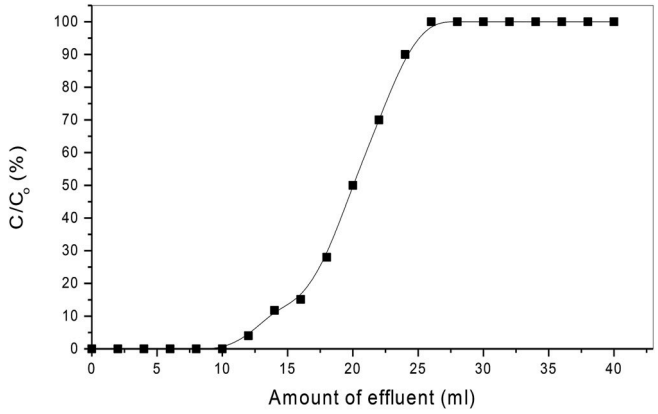

Fig. 10. Breakthrough curve of Mo from the PNCC-1 column by passing MoO_4^{2-} solution (0.01M NaOH, 1 mg Mo/ml) at a flow rate of 1 ml/min.

temperature to reach equilibrium. The ^{99}Mo activities in the aqueous solution before and after equilibration were measured by using the γ-ray spectrometer consisting of an efficient 25% (CANBERRA) HPGe detector, high voltage power supply model CANBERRA 3106D, spectroscopy amplifier coupled with multichannel analyzer, and a gamma-vision software used to analyze the γ-ray spectra. The γ-peak corresponding to the ^{99}Mo at the 739.5 keV ($I_\gamma = 12.2\%$) was counted in 1 ml aliquots. The capacity was determined using the following equation:

$$\textit{Capacity} = \frac{(C_o - C_e)V}{m} \qquad \textit{mmol g}^{-1}$$

where, C_o and C_e are initial and equilibrium concentration of Mo, V is the solution volume and m is the PNCC-1 mass (g).

Secondly, the capacity of Mo was determined under dynamic conditions using a dimension glass column (10 cm long × 0.7 cm i.d) and a glass wool at the bottom, then 0.1 g of PNCC-1 was packed and soaked in 0.01M NaOH. The column was treated by passing 20 ml saline solution (0.9% NaCl), then it was loaded using 0.01M of Mo solution that spiked with 370 kBq (10 μCi) ^{99}Mo per 1 ml of NaOH (0.01M). 1 ml of the loading solution (^{99}Mo) was retained as a reference. 50 ml of the Mo solution was passed through the column by the flow rate 1 ml/min and each 2 ml of the effluent were collected separately and measured the ^{99}Mo activity by HPGe detector. The column was washed with 10 ml of 0.01 M NaOH at a flow rate 1 ml/min. At first, the Mo is adsorbed on the column and when saturated, it descends in the effluent that can be monitored using the ^{99}Mo activity in the effluent. In order to track the sorption behavior, the ratio of the count rate ' C ' of each 1 ml of the effluent to the count rate ' C_o ' of the reference solution (1 ml of the original feed solution). The calculation of capacity was done using the following equation:

$$\textit{Capacity} = \frac{C_o \times V_{50}}{W} \qquad \textit{mmlo g}^{-1}$$

2.5.2. Preliminary studies of PNCC-1 in preparation of ^{99}Mo/^{99m}Tc generator

^{99}Mo was supplied by a fission reaction with a concentration of 1.8–2.8 GBq/ml (48–75 mCi/ml) in 2 M NaOH from the radioisotope production facilities (RPF) and 50 mg/ml molybdenum was added. A glass column of dimension 10 cm long × 0.7 cm (i.d.), with a glass wool at the bottom, was packed with 0.5 g of PNCC-1 in 0.01M NaOH solution. A small piece of glass wool was placed on top of the sorbent bed during a solution flow, then the sorbent material was washed with 20 ml of saline solution (0.9% NaCl). The column was then loaded with 1.48 GBq (40 mCi) of ^{99}Mo solution in 0.01M NaOH. The loaded column was washed directly with 20 ml of a solution of acetone and saline (0.9% NaCl) with a ratio of 3:7 (v/v), respectively. The column was then left sufficient time (24 h) to generate ^{99m}Tc, then it was eluted with a solution of acetone and saline (0.9% NaCl) with a ratio of 3:7 (v/v), respectively, at a flow rate of 1 ml/min. To examine the elution profile, the eluate was collected by a 2 ml aliquot and each fraction was counted by gamma spectrometer. The generator performance was evaluated by periodic elution at 24-h intervals for a duration of 4 days.

2.5.3. Performance of ^{99m}Tc elution

The kinetic desorption of ^{99m}Tc generated on the ^{99}Mo-PNCC-1 column was carried out on the basis of the installation of all the conditions surrounding the elution process (i.e. sorbent mass (0.5 g PNCC-1); column dimensions (10 cm length, 0.7 cm internal diameter) and flow rate (1 ml/min)) except the type of eluent. The ^{99m}Tc was eluted using various concentrations of saline solution (0.05 and 0.9% NaCl) and solutions prepared by adding different acetone volumes to saline solution (1:9, 2:8, 3:7, 4:6 and 5:5, v/v). Appropriate eluent selection is based on the ^{99m}Tc elution yield and its purity (radiochemical, radionuclidic and chemical).

2.5.4. Quality control of ^{99m}Tc eluate

2.5.4.1. Radiochemical purity. The radiochemical purity of the eluted $^{99m}TcO_4^-$ was determined using an ascending paper chromatography technique (Whatman no 1) as a solid phase and 0.9% NaCl solution as a liquid phase. The procedures have been described in a previous work [Amin et al., 2009].

2.5.4.2. Radionuclidic purity. ^{99m}Tc was immediately measured after the separation process and at least two days later using a HPGe detector connected to multichannel analyzer (MCA) to estimate the ^{99}Mo concentration by allowing the ^{99m}Tc decay and then measuring the 739.5 keV peak corresponding to the ^{99}Mo impurity. On the other hand, to measure the ^{99}Mo half-life, it was determined by measuring ^{99m}Tc at 140 keV as a function of decay time.

2.5.4.3. Chemical purity. Possible cerium impurity, resulting from the PNCC-1 matrix was determined in the ^{99m}Tc eluates by using ICP-AES, after making sure the ^{99m}Tc decay out.

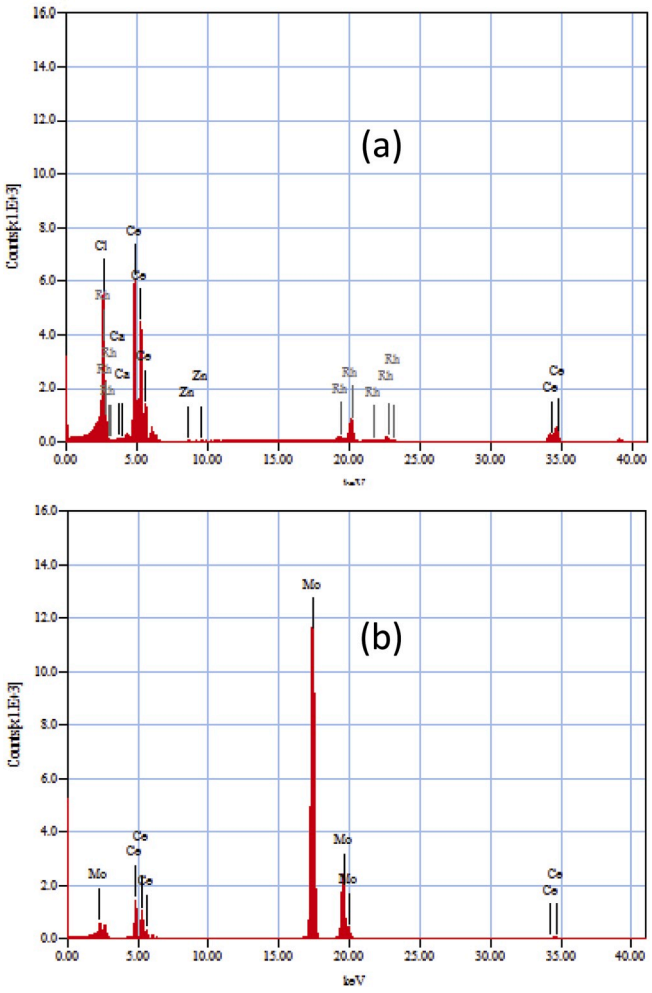

Fig. 11. Elemental analysis using XRF spectrum of (a)poly nano cerium chloride (PNCC-1) and (b)poly nano cerium molybdate (PNCM).

3. Results and discussion

3.1. Characterization of PNCC-1

3.1.1. FTIR spectrum

Fig. 1 (a, b) displays the FTIR spectrum characterizing the absorption of the cerium trichloride heptahydrate (CC) and poly nono cerium chloride (PNCC-1), respectively. The peak at 590 cm^{-1} refers to the presence of Ce–O stretching in both of CC and PNCC-1 [Zhang et al., 2005; McDevitt and Baun, 1964]. Fig. 1 (a, b) shows the strong and broad absorption band around 3400 cm^{-1} due to the presence of vibration absorption of water as well as the peak at 1630 cm^{-1} indicating the presence of hydroxyl group associated with the water molecule bending mode [Lucas et al., 2004]. The weak bands at 1250 and 1400 cm^{-1} indicate that the presence of the C–O group and the C–H bending vibration [Farahmandjou et al., 2016], respectively that appears in Fig. 1 (b) only.

3.1.2. Thermal analysis of PNCC-1

The behavior of $CeCl_3{\cdot}7H_2O$ and PNCC-1 through thermogravimetric analysis (TGA) and differential thermal analysis (DTA) was accomplished and shown in Fig. 2 (a, b). Fig. 2 (b) showed three endothermic peaks centered at 128, 153 and 224 °C, followed by a 536 °C centered exothermic peak. The three broad endothermic peaks could be attributed to removing adsorbed moisture, eliminating the hydroxyl group and decomposing PNCC-1 thermally. Fig. 2 (b), TGA showed weight loss up to ~200OC as follows, 5, 7.8 and 4.2%, respectively, and showed more than one phase in each of the three steps. One step is the oxidation of PNCC-1 at 536 °C to form cerium oxide [Xue et al., 2017], corresponding to the exothermic effect, which appears greater in Fig. 2 (a) than in Fig. 2 (b). This means that the PNCC-1 is thermally more stable than the CC up to 550 °C. Comparing the thermal stability of PNCC-1 with similar compounds, it is found to be even more stable up to 500 °C while poly nano titania is unstable above 300 °C [Chakravarty et al., 2008].

3.1.3. EDX and elemental analysis

PNCC-1 chemical composition was determined using the EDX technique and found to be 48, 28, 13.3, and 8% respectively of cerium, chlorine, oxygen, and carbon, as shown in Fig. 3. The concentration of hydrogen was measured using the elemental analysis and was found to be 1.5%. For each constituent element, the number of mole was calculated and found to be 0.34, 0.79, 0.83, 0.67 and 1.5 respectively for Ce, Cl, O, C and H. The empirical formula of the PNCC-1 was calculated by dividing the number of moles of each constituent element on the least mole number (Ce), and was found to be $CeCl_2O_2C_2H_4$.

3.1.4. X-ray diffraction (XRD) analysis

The crystal structure of PNCC-1 was described using X-ray diffraction as in Fig. 4. The X-ray data were compared to the 32–0199 JCPDS card number. The diffraction broad line of peaks (full width at half maximum of the diffraction peak) could be used to calculate the crystal size by using the Scherer formula:

$$D = \frac{k\lambda}{\beta\, Cos\theta}$$

where D is the crystal size (nm), λ the wavelength of the monochromatic X-ray beam (λ = 1.54°A for CuK_α radiation), β the full width at half maximum diffraction peak (rad.), θ the diffraction angle (°), and k is a constant that varies with the crystal habit and is selected to be 0.9. The size of the crystal is 50 nm. From the findings of Fig. 4, this could be inferred that the poly cerium chloride exists within the scope of the nano scale. During the reaction of cerium chloride heptahydrate with isopropyl alcohol at 160 °C, the formation of multiple cerium chloride products was observed, which was confirmed by a broad endothermic peak in TGA analysis. Furthermore the similarity of the XRD spectrum in this work with the dehydration spectrum of cerium chloride heptahydrate at 170 °C except in few peaks [Xue et al., 2017].

3.1.5. FESEM analysis

The SEM micrograph showed that the size and shape of PNCC-1 was not fully uniform as shown in Fig. 5. The average grain size of PNCC-1 is found to be 50–400 nm by using both SEM and image-j measurements indicating its size scale among crystals, grains and particles. This technique used to determine the crystal size of PNCC-1 is not accurate. Therefore, the XRD technique was used to accurately determine the crystal size. It would be expected that the nano crystal structure of the prepared cerium chloride would have a relatively large surface area,

Table 4
The elution yield of ^{99m}Tc from the ^{99}Mo-PNCC-1 generator using column dimensions (10 cm length × 0.7 cm internal diameter), 0.5g PNCC-1, and different eluents at flow rate 1 ml/min.

Eluents	^{99m}Tc elution yield (%)
0.05% NaCl solution	46.30
0.50% NaCl solution	51.70
0.90% NaCl solution	57.50
10% acetone in 0.9% NaCl solution	55.00
20% acetone in 0.9% NaCl solution	67.50
30% acetone in 0.9% NaCl solution	74.50
40% acetone in 0.9% NaCl solution	69.40
50% acetone in 0.9% NaCl solution	68.30

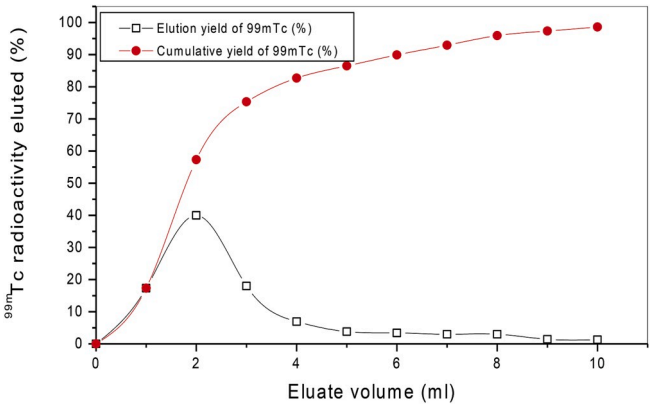

Fig. 12. Elution profile of $^{99m}TcO_4^-$ from $^{99}Mo/^{99m}Tc$ generator.

Table 5
Elution performance of the 1.48 GBq (40 mCi) $^{99}Mo/^{99m}Tc$ generator over a period of 4 days.

Elution No.	Time ofgrowth (h)	Theoretically expected activity of ^{99m}Tc GBq (mCi)	Activity of ^{99m}Tc obtained GBq (mCi)	Elution yield (%)
1	22	1.20 (32.4)	1.10 (30)	75
2	24	0.90 (24.3)	0.85 (23)	74.5
3	24	0.70 (18.9)	0.66 (18)	74
4	24	0.54 (14.7)	0.50 (14)	71

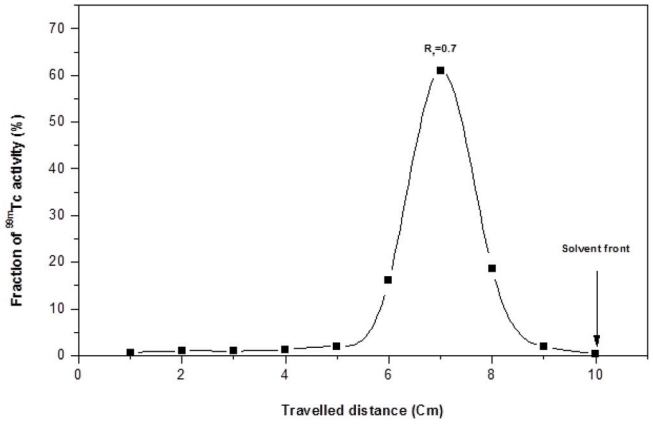

Fig. 13. Radiochromatogram of ^{99mTc} separated from PNCC-1.

which may reflect an increase the ^{99}Mo uptake capacity on PNCC-1. The volume irregularity may be due to the difference in heating distribution in an oil bath and the sudden room temperature cooling after the complete synthesis process so further study is needed to prove this.

3.1.6. Acid-base titration of NPCC-1

Fig. 6 shows that PNCC-1 is an amphoteric ion exchanger and has a point of zero charge (PZC) at pH 3, meaning its surface charge density at pH 3 is equal to zero [kosmulski, 2009]. From the fact that PZC at pH 3, the PNCC-1 has a positively charged surface at pH < 3 and a negatively charged surface at pH > 3. It was found that the Point of zero titration (PZT) was at pH 4.2. The PNCC-1 acts as a cation exchanger (CE) from the point of equivalence (pH 4.2) to the right side and as an anion exchanger (AE) from equivalence point (≤pH 4.2) to the left side as shown in Fig. 6.

3.1.7. Chemical stability

Fig. 7 (a and b) displays the γ-ray spectra of the aqueous solutions 0.01M and 1M NaOH, respectively, as a liquid phase were immediately measured after the separation from the solid phase [^{141}Ce]-PNCC-1. Fig. 7 (c) displays the γ-ray spectrum of the [^{141}Ce]-PNCC-1 as a solid phase, which separated from the 1M NaOH solution and showed the absence of ^{141}Ce peaks (145.44 keV) in the liquid phases. This indicates that the PNCC-1 is chemically stable in the concentrated NaOH solution up to 1M.

3.2. Sorption studies of ^{99}Mo on PNCC-1

The molar ratios of the cerium trichloride heptahydrate to isopropyl alcohol were studied at a certain temperature (90 °C). Table (1) indicates that the highest molybdenum uptake capacity (450 mg Mo/g of PNCC-1) with the highest ^{99m}Tc separation yield was obtained using the molar ratio (1:2). Then, the temperature effect at a constant molar ratio (1:2) was studied as shown in Table (2), which indicated that the maximum molybdenum uptake with the highest separation yield of ^{99m}Tc was achieved at 90 °C. The results indicated that using batch technique, PNCC-1 could be used as the best matrix for the column application based on its ^{99}Mo uptake capacity and ^{99m}Tc separation efficiency. The uptake capacity of Mo and the separation efficiency of ^{99m}Tc were decreased by increasing the IPrOH ratio, this could be due to blocking or covering and decreasing active substitution, exchanging Cl^- sites on the prepared material by increasing the IPrOH ratio. On the other hand, the temperature higher than 90 °C has not great effect on uptake capacity of ^{99}Mo and separation efficiency of ^{99m}Tc

3.2.1. Determination of equilibration time

The ^{99}Mo uptake percentage was studied using PNCC-1 as a function of contact time between the aqueous phase of 0.01 M of Mo labeled by reasonable activity of ^{99}Mo (~10 μCi) in 0.01M NaOH and solid phase of 100 mg PNCC-1 using the batch technique. Fig. 8 shows that the uptake percent of ^{99}Mo on PNCC-1 increased by increasing the contact time to 35 min and remained almost constant (90%) after 20 min.

3.2.2. Effect of NaOH concentration

Fig. 9 shows that the ^{99}Mo Kd values increased from 302 to 2500 ml/g by increasing the NaOH concentration from 0.0001 to 0.01 M, while the ^{99m}Tc Kd values were relatively constant (approximately 100 ml/g). The Kd values of ^{99}Mo are higher than ^{99m}Tc over the entire NaOH concentration range from 0.0001 to 1 M. This could be attributed to the two chloride ions (Cl^-) attached to the PNCC-1 having a tendency to be exchanged by the molybdate molecule MoO_4^{2-} more than pertechnetate $^{99m}TcO_4^-$ at pH > 7 [Cruywagen, 2000; Cruywagen et al., 2002; Greenwood and Earnshaw 1997].

3.2.3. Capacity of PNCC-1

Sorption capacity of PNCC-1, which represents the sorbent ability to retain ^{99}Mo, based on the existence of sorption sites within the matrix or on the exchange reaction between PNCC-1 as a cation exchanger and molybdate MoO_4^{2-} as anion species formed at pH > 7 [Huheey et al., 1996; Wilcox and Gabe 1986]. As the particles of PNCC-1 are in the nano system, and they act as a cation exchanger at pH > 7, which is confirmed by the study of the acid-base titration curve. The static sorption capacity for PNCC-1 was estimated to be 450±27 mg Mo per gram of sorbent (4.68 mmol/g PNCC-1). The value is much higher than that obtained by poly zirconium chloride (215 mg Mo/g ZPC) [Tanase et al., 1997]. This could be attributed to the fact that cerium is a f-block element that can accommodate higher coordination number (8–12) than zirconium, which makes it possible to form more bonding orbital. By comparing our data with the literature data in Table (3), it was observed that PNCC-1 is the highest sorption capacity for ^{99}Mo.

Fig. 10 shows the distribution of loaded Mo by following its activity under the dynamic conditions. It is shown that ^{99}Mo begins to pass out at 12 ml of the loaded Mo referring to the beginning of its breakthrough from the PNCC-1 matrix. The whole Mo added comes out from the

column at about 25 ml. The uptake capacity of Mo is 195 mg/g of PNCC-1.

3.2.4. Reaction mechanism

Fig. 11 (a) displays PNCC-1 constituents using an XRF analysis that indicates the presence of 55 and 45% of cerium and chlorine respectively prior to its reaction with molybdate ions. Fig. 4 (b) indicates the presence of cerium with mostly constant percentage (48%), while the absence of chlorine, which it was replaced by the molybdenum with a percent 52% post the ion exchange reaction. This confirms that the ions of molybdenum MoO_4^{2-} substitute the chloride ions in PNCC-1 during the exchange reaction as the following mechanism:

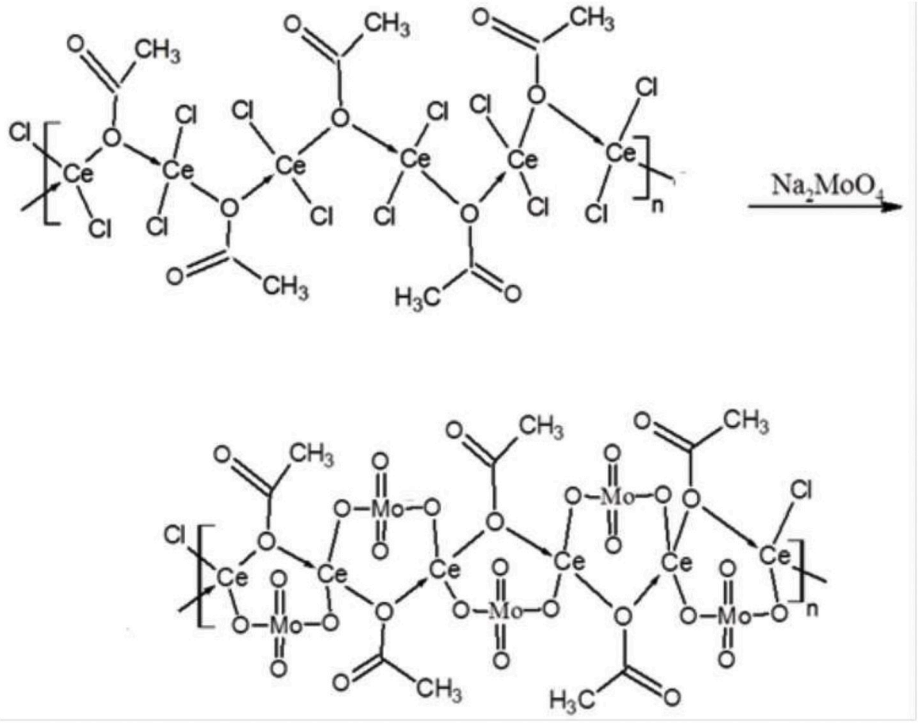

3.2.5. Performance of ^{99m}Tc elution

Table (4) displays the elution yield of ^{99m}Tc using different eluents. It can be observed that increasing the concentration of saline solution from 0.05 to 0.9% NaCl, the elution yield of ^{99m}Tc increases from 46.3 to 57.5%. However, the elution yield using saline solutions does not give the desired values. Elution yield increased from 55 to 75% by increasing the percentage of acetone from 10 to 30% in saline solution, because acetone is one of the most sensitive solvents for a number of elements and is easily water miscible [Robinson, 1960]. MoO_4^{2-} is more closely related to PNCC-1 than TcO_4^- because of MoO_4^{2-} has bi-bonding, while TcO_4^- mono-bonding with PNCC-1. Using the high percentage of acetone such as 40% and 50%, the elution yield decreased to 69.4 and 68.3% may be due to the high concentration of acetone, making it relatively water-immiscible, which decreases its sensitivity to TcO_4^-.

3.2.6. Preliminary study to use PNCC-1 for the $^{99}Mo/^{99m}Tc$ generator

The optimum conditions obtained during a study the PNCC-1sorption properties were used to prepare the $^{99}Mo/^{99m}Tc$ generator by loading the relatively high activity of ^{99}Mo ~1.48 GBq (40 mCi) onto the PNCC-1 matrix in the glass column (10 cm length x 0.7 cm i.d). Fig. 12 shows the elution profile of ^{99m}Tc, indicating that 90% of the total $^{99m}TcO_4^-$ available in the first 6 ml of acetone to saline solution (0.9% NaCl) of a ratio of 3:7 (v/v). Table (5) explains the results of the elution of ^{99m}Tc over a 4-day period and its elution yield was approximately 75% by the sequential elution. It was observed that generator yields ranged from 78 to 80% ^{99m}Tc of the theoretical yields over a period of four days. The eluted ^{99m}Tc was studied from the point of view of radiochemical and radionuclidic purity in order to investigate their compliance with nuclear medicine requirements as the following steps:

3.2.6.1. Radiochemical purity. Fig. 13 shows the radiochromatogram of the separated ^{99m}Tc radioactivity using Whatman No. 1 ascending paper chromatography. A single peak was obtained with R_f-value of 0.7, which related to pertechnetate anions ($^{99m}TcO_4^-$). The radiochemical purity was found to be 98.0±0.2% [IAEA, 2008; Amin et al., 2009].

3.2.6.2. Radionuclidic purity. Gamma-ray spectrometry and radioactive decay measurements were done using a multichannel analyzer and NaI (Tl) scintillation counter to verify the radionuclidic purity of the eluted solutions that has a half-life ~ 6 h corresponding to ^{99m}Tc with 99.99±0.001%.

3.2.6.3. Chemical purity. The concentration of cerium in the eluate of ^{99m}Tc didn't exceed 0.1–1 μg/ml. These values are suitable for medical applications and below the permissible level (10 ppm) [Galle and Masse 1982]. On the other hand, in order to extract acetone from the eluate of ^{99m}Tc, the literature data revealed that the dibasic potassium phosphate (K_2HPO_4) could be used to separate the acetone into even 100%, and that it is used safely as a buffering agent [Xie et al., 2018].

4. Conclusion

A new polymeric nanomaterial was successfully prepared as a prospective sorbent material for $^{99}Mo/^{99m}Tc$ generator, due to the high capacity of molybdenum on PNCC-1 (450±27 mg Mo/g PNCC-1) with separation yield of ^{99m}Tc (55%) using batch technique. It was

determined the chemical composition of PNCC-1 using the EDX technique. It was found that the empirical formula of PNCC-1 was $CeCl_2O_2C_2H_4$ and verified by the study of IR, TGA and DTA. The exchange reaction was carried out by molybdate (MoO_4^{2-}) replacement of chloride ions (Cl^-) on PNCC-1 matrix, which was confirmed by the XRF analysis before and after the exchange process. The morphology structure of PNCC-1 was investigated using XRD and SEM, which indicates that its nano-scale crystallinity with a variable range of 50–400 nm could be due to the difference in the distribution of heating in an oil bath, so further study will be carried out in the following work. Preliminary studies on the PNCC-1 matrix were performed using the glass column to prepare the $^{99}Mo/^{99m}Tc$ generator for the absorbing capacity of Mo (195±11 mg/g adsorbent) with an elution yield of approximately 75% of ^{99m}Tc. Quality control on eluted ^{99m}Tc was studied and found to be acceptable for radionuclidic and radiochemical purity.

Declaration of competing interest

The authors whose names are listed immediately below certify that they declare that they have no conflict of interest.

CRediT authorship contribution statement

M.I. Aydia: Writing - original draft, Writing - review & editing, Supervision. **K.M. El-Azony:** Data curation, Writing - original draft, Writing - review & editing, Supervision. **T.Y. Mohamed:** Writing - review & editing, Supervision. **I.M. Shahin:** Writing - review & editing, Supervision.

Acknowledgments

The authors are grateful to the International Atomic Energy Agency for funding our work through the IAEA Coordinated Research Project No: F22068.

References

Amin, A.M., El-Azony, K.M., Ibrahim, I., 2009. Application of $^{99}Mo/^{99m}Tc$ alumina generator in the labeling of metoprolol for diagnostic purposes. J. Label. Compd. Radiopharm. 52, 467-272.
Ballinger, J.R., 2010. ^{99}Mo shortage in nuclear medicine: crisis or challenge? J. Label. Compd. Radiopharm. 53, 167–168.
Boyd, R.E., 1982. Technetium-99m generators-the available options. Int. J. Appl. Radiat. Isot. 33, 801–810.
Boyd, R.E., 1997. The gel generator: a viable alternative source of ^{99m}Tc for nuclear medicine. Appl. Radiat. Isot. 48, 1027–1033.
Cecchin, D., Zucchetta, P., Faggin, P., Bolla, E., Bui, F., 2010. $^{99}Mo/^{99m}Tc$ generator shortage. J. Nucl. Med. 51, 14N–5N.
Chakravarty, R., Bahadurb, J., Lohara, S., Sarmad, H.D., Senb, D., Mishrac, R., Chakrabortya, S., Dash, A., 2019. Solid state synthesis of mesoporous alumina: a viable strategy for preparation of an advanced nanosorbent for 99Mo/99mTc generator technology. Microporous Mesoporous Mater. 287, 271–279.
Chakravarty, R., Ram, R., Dash, A., Pillai, M.R.A., 2012. Preparation of clinical-scale $^{99}Mo/^{99m}Tc$ column generator using neutron activated low specific activity ^{99}Mo and nanocrystalline γ-Al_2O_3 as column matrix. Nucl. Med. Biol. 39, 916.
Chakravarty, R., Shukla, R., Gandhi, S., Ram, R., Dash, A., Venkatesh, M., Tyagi, A.K., 2008. Polymer embedded nanocrystalline titania sorbent for ^{99}Mo-^{99m}Tc generator. J. Nanosci. Nanotechnol. 8, 4447.
Chakravarty, R., Ram, R., Mishra, R., Sen, D., Mazumder, S., Pillai, M.R.A., Dash, A., 2013. Mesoporous alumina (MA) based double column approach for development of a clinical scale $^{99}Mo/^{99m}Tc$ generator using $(n,\gamma)^{99}Mo$: an enticing application of nanomaterial. Ind. Eng. Chem. Res. 52, 11673–11684.
Chakravarty, R., Shukla, R., Ram, R., Tyagi, A.K., Dash, A., Venkatesh, M., 2010. Practicality of tetragonal nano-zirconia as a prospective sorbent in the preparation of $^{99}Mo/^{99m}Tc$ generator for biomedical applications. Chromatographia 72, 875–884.
Chattopadhyay, S., Das, S.S., Alam, M.N., 2017. Madhusmita, Preparation of $^{99}Mo/^{99m}Tc$ generator based on cross-linked chitosan polymer using low-specific activity $(n,\gamma)^{99}Mo$. J. Radioanal. Nucl. Chem. 313, 647–653.
Cruywagen, J.J., 2000. Protonation, oligomerization, and condensation reactions of vanadate(V), 20 molybdate(VI), and tungstate(VI). Adv. Inorg. Chem. 49, 127–182.
Cruywagen, J.J., GDraaijer, J.B., BHeyns, E.A., Rohwerruywagen, A., 2002. Thermodynamic quantities. Inorg. Chim. Acta. 331, 322–329.
Eckelman, W.C., Coursay, B.M., 1982. Technetium-99m special issue. Int. J. Appl. Radiat. Isot. 33 (10), 793–951.
Eckelman, W.C., 2009. Unparalleled contribution of technetium-99m to medicine after 5 decades. J. Am. Coll. Cardiol Imaging 2, 364–368.
Evans, J.V., Shying, M.E., 1984. Zirconium Molybdate Gel as a Generator for Technetium-99m. Australian Atomic Energy Commission. AAEC/E–599.
Farahmandjou, M., Zarinkamar, M., Firoozabadi, T.P., 2016. Synthesis of Cerium Oxide (CeO_2) nanoparticles using simple CO-precipitation method. Revista Mexicana de Física 62, 496–499.
Galle, P., Masse, R. (Eds.), 1982. Radionuclides Metabolism and Toxicity. Masson, Paris.
Gould, P., 2009. Medical isotope shortage reaches crisis level; robust solutions sought urgently to shore up fragile supply chain. Nature 460 (725), 312–313.
Greenwood, N.N., Earnshaw, A., 1997. Chemistry of the Elements, second ed.
Hasan S., 2014. Preparation of Chitosan-Based Microporous Composite Material and its Applications. U S Patent Publication, US 8,911,695 B2. Pub. Date: Dec. 16, 2014.
Huheey, J., Keiter, E.A., Keiter, R.L., 1996. Inorganic Chemistry. De Boeck Universite, Bruxelles, p. 50.
International Atomic Energy Agency (IAEA), 2008. Technetium-99m Radiopharma Ceuticals, Manufacture of Kits. Tech. Rep. Series No. 466, Vienna.
Kosmulski, M., 2009. pH-dependent surface charging and points of zero charge. IV. Update and new approach. J. Colloid Interface Sci. 337 (2), 439–448.
Lagunas-Solar, M.C., 1993. Production of ^{99m}Tc and ^{99}Mo for Nuclear Medicine Applications via Accelerators as an Option to Reactor Method, Presented at the 18th Annual Conference of the Australian Radiation Protection Society, Held 6-8 October. University of Sydney, Australia.
Lagunas-Solar, M.C., Kiefer, P.M., Carvacho, O.F., Lagunas, C.A., Cha, Y.A.P.O., 1991. Cyclotron production of NCA 99mTc and 99Mo. An alternative non-reactor supply source of instant 99mTc and 99Mo→99mTc generators. J. Appl. Rad. Isot. 42 (7), 643–657.
Lee, S.K., Beyer, G.J., Lee, J.S., 2016. Development of industrial-scale fission 99Mo production process using low enriched uranium target. Nucl. Eng. Tech. 48 (3), 613–623.
Lucas, S., Champion, E., Bernache-Assollant, D., Leroy, G., 2004. Rare earth phosphate powders RePO4·nH2O (Re=La, Ce or Y) II. Thermal behavior. J. Solid State Chem. 177 (4–5), 1312–1320.
McDevitt, N.T., Baun, W.L., 1964. Infrared absorption study of metal oxides in the low frequency region (700-240 cm^{-1}). Spectrochim. Acta 20 (5), 799–808.
Molinsky, V.J., 1982. A review of ^{99m}Tc generator technology. Int. J. Appl. Radiat. Isot. 33 (10), 811–819.
Monroy-Guzman, F., Arriola, S.H., Ortega, A.I., Díaz, A.L.V., Cortes, R.O., 2007. Determination of Mo, W and Zr in molybdates and tungstates of zirconium and titanium. J. Radioanal. Nucl. Chem. 271 (3), 523–532.
Nuclear Energy Agency (NEA), 2018. Medical Isotope Supply Review: 99Mo/99mTc Market Demand and Production Capacity Projection 2018-2023 Period, 99Mo Topical Meeting, Knoxville 23-26 September 2018. OECD Publishing, Paris.
Parrington, J.R., Knox, H.D., Breneman, E.M., Baum, E.M., Feiner, F., 1996. Nuclides and Isotopes, fifteenth ed. Lockheed Martin/GE Nuclear Energy, Schenectady, NY).
Perkins, A.C., Vivian, G., 2009. Molybdenum supplies and nuclear medicine services. Nucl. Med. Commun. 30 (9), 657–659.
Pupillo, G., Esposito, J., Haddad, F., Michel, N., Gambaccini, M., 2015. Accelerator-based production of ^{99}Mo: a comparison between the $^{100}Mo(p, x)$ and $^{96}Zr(\alpha, n)$ reactions. J. Radioanal. Nucl. Chem. 305, 73–78.
Robinson, J.W., 1960. Effect of organic and aqueous solvents on flame photometric emission and atomic absorption spectroscopy. Anal. Chim. Acta 23, 479-478.
Scholten, B., Lambrecht, R.M., Cogneau, M., Vera Ruiz, H., Qaim, S.M., 1999. Excitation functions for the cyclotron production of ^{99m}Tc and ^{99}Mo. J. Appl. Rad. Isot. 51 (1), 69–80.
Seaborg, G.T., Segrè, E., 1939. Nuclear isomerism of element 43. Phys. Rev. 55, 808–814.
Saptiama, I., Kaneti, Y.V., Suzuki, Y., Tsuchiya, K., Fukumitsu, N., T Sakae, T., Kim, J., Kang, Y.M., Ariga, K., Yamauchi, Y., 2018. Template-free fabrication of mesoporous alumina nanospheres using post-synthesis water-ethanol treatment of monodispersed aluminium glycerate nanospheres for molybdenum adsorption. Small 14 (21), 1800474.
Takács, S., Szucs, Z., Tárkányi, F., Hermanne, A., Sonck, M., 2003. Evaluation of proton induced reactions on ^{100}Mo: new cross sections for production of ^{99m}Tc and ^{99}Mo. J. Radioanal. Nucl. Chem. 257 (1), 195–201.
Tanase, M., Tatenuma, K., Ishikawa, K., Kurosawa, K., Nishino, M., Hasegawa, Y., 1997. ^{99m}Tc generator using a new inorganic polymer adsorbent for (n,γ) ^{99}Mo. Appl. Rad. Isot. 48 (5), 607–611.
Wilcox, G.D., Gabe, D.R., 1986. The role of molybdates in corrosion prevention. Corrosion Rev. 6 (4), 327–365.
Xie, S., Song, W., Fu, C., Yi, C., Qiu, X., 2018. Separation of acetone: from a water miscible system to an efficient aqueous two-phase system. Separ. Purif. Technol. 192, 55–61.
Xue, S., Wu, W., Bian, X., Wu, Y., 2017. Dehydration, hydrolysis and oxidation of cerium chloride heptahydrate in air atmosphere. J. Rare Earths 35, 1156–1163.
Zhang, Z., Kleinstreuer, Donohue, J.F., Kim, C.S., 2005. Comparison of micro and nano-size particle depositions in a human upper airway model. J. Aerosol Sci. 36, 211–233.
Zolle, I., 2007. Technetium-99m Radiopharmaceutical; Preparation and Quality Control in Nuclear Medicine. Springer, Berlin.